TECH LIBRARY KAFB, N
0067174
TN 4360 10704
NATIONAL ADVISORY COMMITTEE

ON WAVE ATTENUATION IN A TRANSONIC WIND

NATIONAL ADVISORY COMMITTEE FOR AERONAUTICS

TECHNICAL NOTE 4360

MEASUREMENTS OF THE EFFECTS OF WALL OUTFLOW AND POROSITY ON WAVE ATTENUATION IN A TRANSONIC WIND TUNNEL WITH PERFORATED WALLS

By Joseph M. Spiegel, Phillips J. Tunnell,
and Warren S. Wilson

SUMMARY

An investigation was made in a 5- by 5-inch transonic test section of the wave attenuating capabilities of a variety of perforated-wall configurations both with and without the use of outflow. The evaluation was made by comparing static-pressure measurements on a body of revolution from tests in a 5- by 5-inch test section with those from tests of the identical model in the Ames 2- by 2-foot transonic wind tunnel.

The test results indicated that reflected disturbances could be minimized through the Mach number range tested (M = 1.0 to 1.36) either by varying the outflow through walls of constant porosity, or by varying the wall porosity at constant low outflow. At sonic speed only a very low-porosity wall yielded minimum interference.

INTRODUCTION

Perforated walls are used in transonic wind tunnels primarily to attenuate the reflection of model-induced disturbances from the walls at supersonic speeds. The attenuation of these disturbances is dependent primarily on the permeability of the perforated walls and is influenced by the interaction of the disturbances with the boundary layer (refs. 1, 2, and 3). Wall permeability, defined as the capacity of a porous boundary to pass fluid, is dependent upon many factors of which the primary ones are porosity and initial outflow. If a porous wall is to be effective in canceling disturbances, the boundary layer must be sufficiently thin. This can be insured by inducing an initial outflow through the perforated walls before imposing the model disturbance field (ref. 3).

The purpose of the investigation presented in this paper was to determine the relative advantages of two different methods in attenuating model-induced disturbances in the Mach number range from 1.0 to 1.36. The first method was to maintain a constant-porosity wall and vary the permeability by varying the initial outflow. The second technique was to vary the permeability by varying the porosity with the initial outflow held small and constant.

NOTATION

a	orifice position from nose of body
d	body diameter
l	body length
m	$\frac{\text{mass flow through walls}}{\text{mass flow through tunnel}}$
M	Mach number
p	static pressure of free stream
p_c	static pressure in plenum chamber enclosing test section
p_l	static pressure on body in 5- by 5-inch test section
p_r	static pressure on body in 2- by 2-foot test section
p_t	total pressure
p_w	static pressure at wall
q	dynamic pressure of free stream
R	permeability factor, $R = \frac{2v/V}{(p_w-p_c)/q}$
v	velocity component normal to free-stream flow
V	free-stream velocity
β	$\sqrt{M^2-1}$
θ	wall angle, deg (Convergence in downstream direction is negative.)
α	flow angle, $\tan^{-1}\frac{v}{V}$

EQUIPMENT

The Test Facility

The transonic test facility employed for these experiments is a blowdown to atmosphere type which utilizes a single-jack variable-geometry convergent-divergent nozzle to generate supersonic Mach numbers up to 1.36. (A detailed description of this type of nozzle is given in ref. 4.)

The perforated test section is approximately 5 inches square in cross section and 9-7/8 inches long. The nozzle, test section, and diffuser entry are shown in figure 1. The vertical side walls of the test section were always maintained parallel to the air stream, but the top and bottom walls in some cases were converged or diverged by means of the jack mechanism shown in the figure.

Test-Section Configurations

The perforated test-section configurations were of two general types. One utilized thin perforated plates for the tunnel side walls and is shown in figure 1; the other is the same as that shown in figure 1 except that the side walls were relatively thick and no suction (outflow) was used other than that provided by the ejector action of a step at the junction of the test section and diffuser (see ref. 4).

The details of the perforated walls tested are shown in figures 2(a), 2(b), and 2(c). Figure 2(a) shows the 12.4- and 24.4-percent open-area thin walls with perforations normal to the surface. Figure 2(b) shows the thin walls with holes slanted 30° to the surface and into the air stream. Filling alternate longitudinal rows of holes reduced the original open area of 12.5 percent to 6.2 percent, and filling alternate transverse rows further reduced the open area to 3.1 percent. The thick walls, shown in figure 2(c), had triangular-shaped perforations and were built of alternate solid and serrated longitudinal rails. The serrated rail thickness was milled to obtain a range of decreasing porosities. For these walls the porosities ranged from 9.6 to 0.60 percent.

Instrumentation

To appraise the quality of flow in the empty test section a translatable axial tube was used which extended from the settling chamber through the test section and into the diffuser. Orifices were provided on the axial tube to measure the static pressure in the nozzle and test section. Total pressure was obtained from the static pressure measured in the settling chamber. To determine the mass flow removed by the auxiliary suction equipment a standard ASME sharp-edged orifice plate with radius taps was used.

Models

Three different types of models were used to generate disturbances: (1) wing-body, (2) body of revolution, fineness ratio 12 (RM 12), and (3) cone-cylinder. Figures 3(a) and 3(b) show the two wing-body models.

These models are geometrically similar forward of the wing trailing edge. The body of revolution (RM 12) is shown in figure 3(c). The two cone-cylinder models shown in figure 3(d) were essentially identical except for the cylinder length and the location of the static-pressure orifices.

TESTS

The strength of reflected disturbances was investigated by measuring pressures along the test bodies at 0° angle of attack for Mach numbers from 0.60 to 1.36 in both the 5- by 5-inch and the 2- by 2-foot test sections.

Pressures on the bodies were measured with the plenum-chamber pressure as the reference. The body pressures were referred to free-stream static pressure by subtracting the difference between the average test-section and the plenum-chamber pressures obtained from the tunnel-empty calibrations. In equation form

$$p_l - p = (p_l - p_c)_{\text{model test}} - (p - p_c)_{\text{tunnel-empty test}}$$

For all tunnel-empty tests the maximum variation in free-stream Mach number was ±0.010 along the test-section center line.

RESULTS AND DISCUSSION

Analytic Considerations

The need for varying permeability with Mach number for elimination of blockage effects at subsonic speeds and of reflected disturbances at supersonic speeds is predicted by theory. A permeability factor can be defined as (ref. 1),

$$R = \frac{2v/V}{(p_w - p_c)/q} = \frac{2 \tan \alpha}{(p_w - p_c)/q} \qquad (1)$$

At subsonic speeds it has been shown by means of linear theory that the blockage correction on a small slender three-dimensional body at zero lift can be minimized if the permeability factor is equal to 0.83β (ref. 5). Goodman (ref. 1) states that at supersonic speeds the permeability factor should equal β for complete cancellation of weak two-dimensional oblique shock waves. Hence, both subsonic and supersonic theories predict a need for variable permeability with Mach number. In figure 4 is shown the relationship between the flow angle and pressure coefficient required at the wall for two-dimensional wedges and three-dimensional bodies of revolution over a range of Mach numbers. The slope of the straight lines indicates the permeability required to cancel weak two-dimensional waves at various Mach numbers, that is, $R = \beta$. The points labeled "ogive bow

wave" were obtained from measurements (from schlieren photographs taken in the 2- by 2-foot transonic wind tunnel) of the bow-wave angle at the equivalent wall position of the 5- by 5-inch test section. This angle and the corresponding Mach number were used to determine the pressure coefficient and turning angle from oblique-shock-wave theory. The leaders indicate the curve of $R = \beta$ to which the points apply. Note that with increasing Mach number a higher permeability is required to cancel two-dimensional shock waves. For the three-dimensional case the flow permeability curves required at wall stations corresponding to the longitudinal pressure field of the model have been calculated and plotted for the RM 12 and ogive bodies of revolution by linear theory for Mach numbers of 1.1. and 1.2, respectively. It is shown that near the nose of the bodies there is close agreement with the two-dimensional requirements, but away from the nose there is disagreement which indicates that a more open wall is needed. (The 20- and 50-percent body length stations are identified on the curves.) Although not shown for other Mach numbers, these curves for bodies of revolution rotate to indicate a higher permeability requirement with increased Mach number. Plots of this type for cone-cylinders and cone-ogive-cylinders at several blockage ratios are presented in reference 6.

Experimental Effect of Outflow and Porosity on Reflected Disturbances

Wing-body model; 0.6-percent blockage.- Typical plots of the variation of pressure coefficient with Mach number at two orifices of the small wing-body model are presented in figure 5. For these tests the thin-walled test section with normal perforations having 12.4- and 24.4-percent porosity was used. Results at low and high outflow values are compared with those from 2- by 2-foot transonic wind-tunnel tests. It is to be noted that peak disturbances pass over an orifice at a lower Mach number as the strength of the reflection decreases.

Figure 5 shows that at supersonic Mach numbers up to 1.15 the reflected disturbances are least with high outflow at 12.4-percent porosity. At the higher speeds, however, the disturbances were smallest with low outflow at 12.4-percent porosity. This illustrates that outflow can be used to change the permeability of the walls and hence to reduce the strength of reflected disturbances over a range of Mach numbers.

In figure 6 is shown a summary plot of wave-reflection strength as a function of outflow for the disturbance waves indicated in figure 5. Consider first the wing-wave disturbances. The data show that the use of outflow produces a marked reduction in strength at constant wall porosity. It is further shown that the lower porosity resulted in lower reflection strength and considerably less outflow, and this trend suggests that even better results would be obtained with a still lower porosity than 12.4 percent, particularly at Mach numbers of about 1.1.

The plots for the bow wave in figure 6 indicate that increasing outflow can convert the reflected disturbance from an expansion to a compression wave. The data also indicate that low interference can be obtained by decreasing the outflow with increasing Mach number at constant porosity.

Wing-body model; 1.35-percent blockage.- In figure 7 is shown the variation of pressure coefficient at three body orificies with Mach number for the large wing-body model tested in the 24.4-percent open-area test section at low and high outflow. Data for tests at subsonic speeds in the 12.4-percent open-area test section are also presented. Figure 8 is a summary plot which shows the variation in reflection strength with outflow for the waves designated in figure 7. The effects of varying outflow are similar to those shown for the small model.

RM 12 model; 0.35-percent blockage.- In figures 9(a) and 9(b) is shown a comparison of the effect of low and high outflow on the pressure distribution of the RM 12 at Mach numbers of 1.00 to 1.14. The plots show that at Mach numbers above unity increased outflow for either porosity reduced the magnitude of the interference. At $M = 1$ none of the data agree very well with the data obtained in the 2- by 2-foot transonic wind tunnel.

In figure 10 is shown a plot against Mach number of the maximum difference between the test data from the 5- by 5-inch and the 2- by 2-foot test sections for the range of body stations tested. The data shown are presented at outflow values corresponding to least average interference. This plot clearly indicates that the 24.4-percent walls are too open even at the high Mach numbers for the highest outflow tested. The data for the 12.4-percent walls indicate the need for decreasing outflow with increasing Mach number at constant porosity.

In figure 11 are plotted pressure distributions for the thick walls at the porosity which indicated least interference at each Mach number presented. The point to note is the usefulness of varying the porosity with Mach number. A comparison of the data with the 2- by 2-foot wind-tunnel tests shows that reasonable agreement was accomplished by increasing the porosity with increases in Mach number. At $M = 1.0$ and 1.14 the maximum and minimum porosities investigated are shown to illustrate the magnitude of the reflected disturbances in an off-design condition.

In figure 12 is shown a summary plot against Mach number of the maximum difference between the test data from the 5- by 5-inch and 2- by 2-foot wind tunnels. For the thick walls the variable-porosity results as well as data for a constant porosity of 7.1 percent are presented.

Three significant results are shown in figure 12. First, it is shown that at constant low outflow varying porosity with Mach number provides a decided improvement over constant porosity at constant low

outflow. Second, for this model configuration and size, varying porosity at low constant outflow is virtually as satisfactory as maintaining constant porosity and varying outflow. Third, only low porosity provides the least interference near a Mach number of 1.

In figure 13 is shown a summary plot of the variation of open area required for least interference as a function of Mach number. Data for the RM 12 model are shown up to $M = 1.18$, where the wave reflection influences only the last orifice. The data indicate the need for porosity variation with Mach number. The theoretical line, presented merely to indicate the qualitative similarity in trend, is based on the assumption that porosity for cancellation is proportional to β, as discussed previously. The theoretical curve is adjusted to coincide with the experimental curve at $M = 1.08$.[1]

Cone-cylinder; 0.35-percent blockage.- In figure 14 is shown the effect of outflow, through the 24.4-percent open-area walls, on the pressure distribution of a cone-cylinder at supersonic speeds. Outflow is shown to be beneficial at supersonic Mach numbers above 1.04.

In figure 15 is shown the effect of porosity variation for the slant holes on the pressure distribution of the cone-cylinder at supersonic speeds. The trend of these data is in agreement with the increasing porosity requirement with Mach number predicted by theory. The similarity of distributions between the 12.5-percent porosity data of figure 15 and the 24.4-percent data of figure 14 leads to the conclusion that both walls are of nearly the same permeability. This is not surprising since it is shown in reference 7 that the flow resistance of holes slanted 30° to the stream is much less than that for normal holes.

SUMMARY OF RESULTS

Tests of the wave attenuating capabilities of a variety of perforated-wall transonic test sections with wall outflow and/or porosity (open-to-total area ratio) as the primary parameters at Mach numbers up to 1.36 indicated:

1. For walls of high porosity (12 to 25 percent), the use of outflow through the perforated walls at Mach numbers above 1 generally reduced peak reflection strengths markedly at fixed values of porosity.

2. All tests corroborated theoretical predictions that permeability should increase with increasing supersonic Mach number in order to minimize wave reflections for the particular models tested.

[1]Permeability, rather than porosity, would have been a more appropriate ordinate, but permeability of the thick walls was not determined.

3. Between Mach numbers of about 1.04 and 1.36 varying the outflow can produce the necessary variation in permeability if the wall porosity is suitably chosen. This method of permeability control requires a larger outflow quantity than a combination of variable porosity and variable outflow.

4. At sonic free-stream velocity for a small contoured body of revolution, varying outflow was essentially ineffective in reducing interference. Only nearly closed walls at low outflow yielded minimum interference.

Ames Aeronautical Laboratory
National Advisory Committee for Aeronautics
Moffett Field, Calif., June 6, 1958

REFERENCES

1. Goodman, Theodore R.: The Porous Wall Wind Tunnel. Part III - The Reflection and Absorption of Shock Waves at Supersonic Speeds. Rep. No. AD-706-A-1, Cornell Aero. Lab., Inc., 1953.

2. Spiegel, Joseph M., and Tunnell, Phillips J.: An Analysis of Shock-Wave Cancellation and Reflection for Porous Walls Which Obey an Exponential Mass-Flow Pressure-Difference Relation. NACA TN 3223, 1954.

3. Goethert, B. H.: Flow Establishment and Wall Interference in Transonic Wind Tunnels. AEDC-TR-54-44, Arnold Engr. Dev. Ctr., June 1954.

4. Spiegel, Joseph M., and Lawrence, Leslie F.: A Description of the Ames 2- by 2-Foot Transonic Wind Tunnel and Preliminary Evaluation of Wall Interference. NACA RM A55I21, 1956.

5. Baldwin, Barrett S., Jr., Turner, John B., and Knechtel, Earl D.: Wall Interference in Wind Tunnels With Slotted and Porous Boundaries at Subsonic Speeds. NACA TN 3176, 1954.

6. DuBose, H. C.: Experimental and Theoretical Studies on Three-Dimensional Wave Reflection in Transonic Test Sections. Part II: Theoretical Investigation of the Supersonic Flow Field About a Two-Dimensional Body and Several Three-Dimensional Bodies at Zero Angle of Attack. AEDC-TN-55-43, Arnold Engr. Dev. Ctr., 1956.

7. Chew, W. L.: Experimental and Theoretical Studies on Three-Dimensional Wave Reflection in Transonic Test Sections. Part III: Characteristics of Perforated Test-Section Walls With Differential Resistance to Cross-Flow. AEDC-TN-55-44, Arnold Engr. Dev. Ctr., 1956.

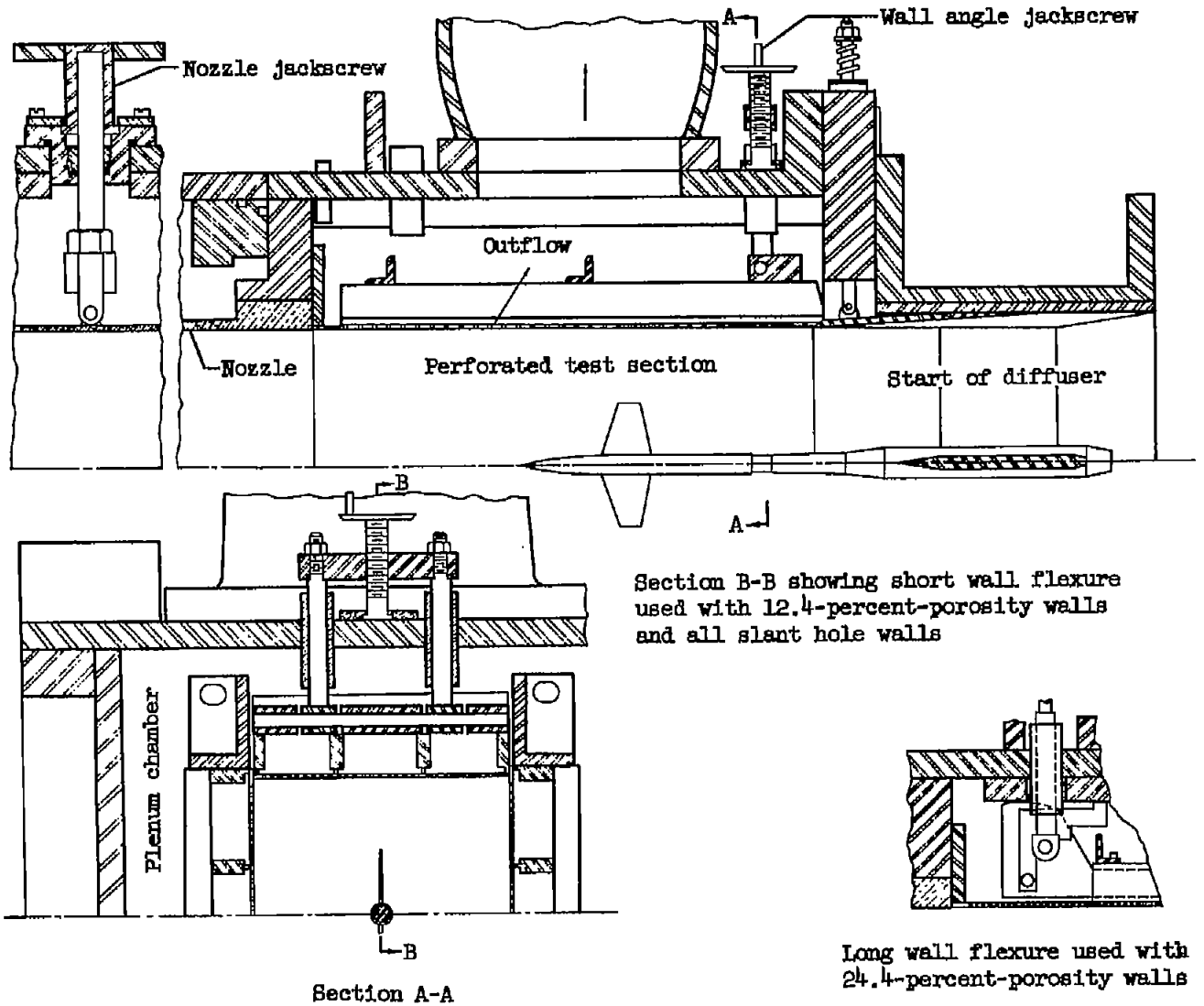

Figure 1.- The high-speed region of the 5- by 5-inch transonic test facility.

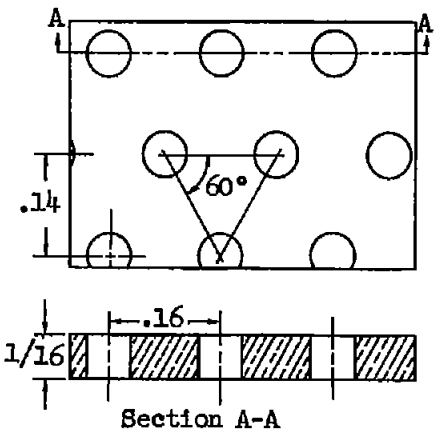

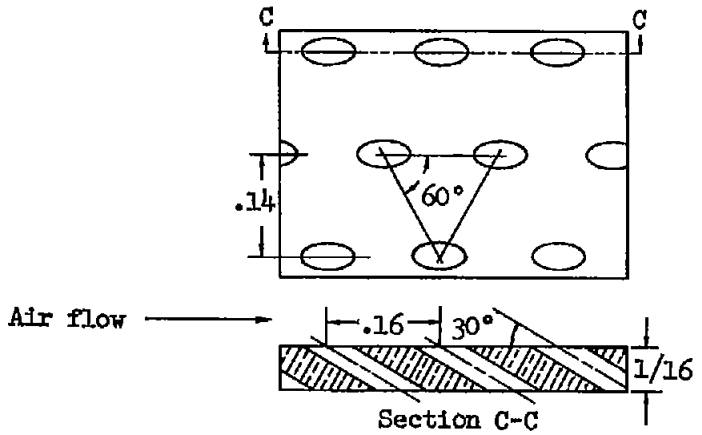

(b) Slant hole walls; 0.0420-inch-diameter drill size.

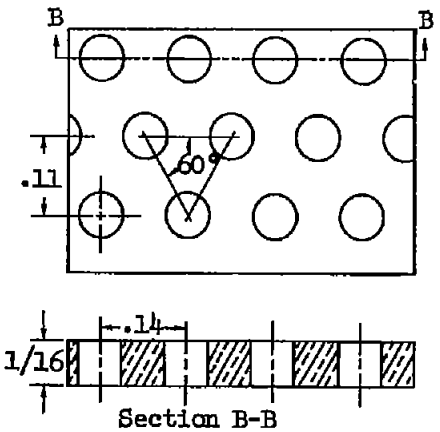

(a) Thin walls; 12.4- and 24.4-percent porosity, 1/16-inch normal hole diameter.

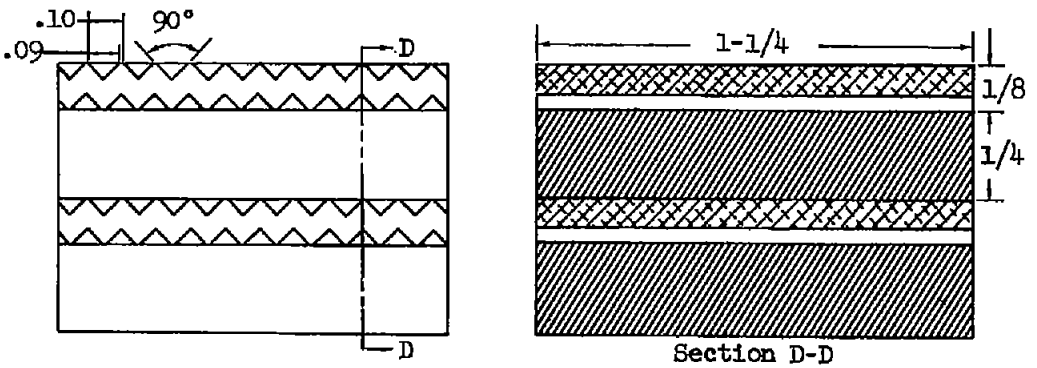

(c) Thick walls; 9.6-percent porosity shown.

Figure 2.- Geometry of the perforated wall porosity (all dimensions in inches).

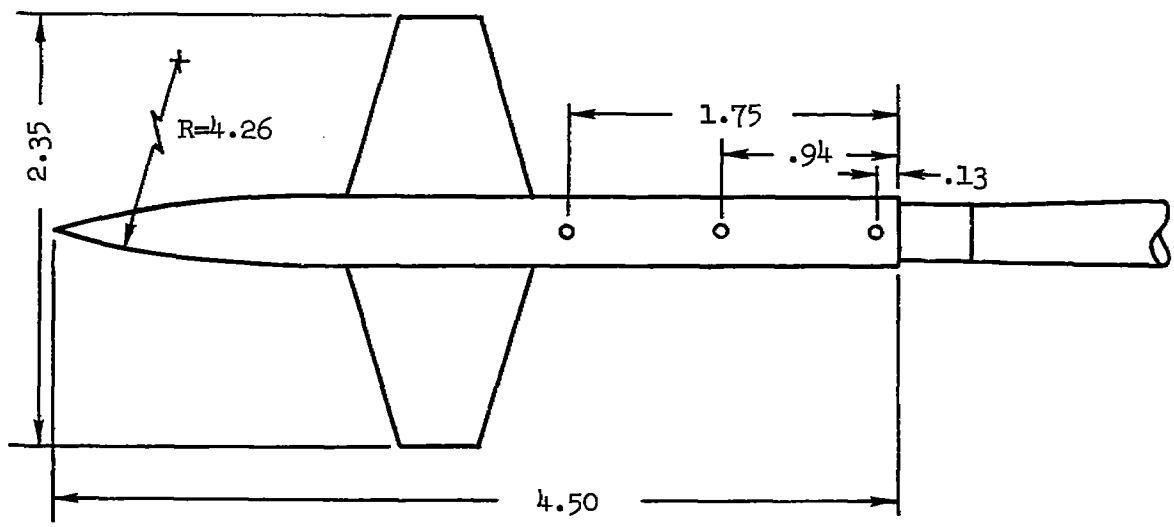

(a) Small wing-body model.

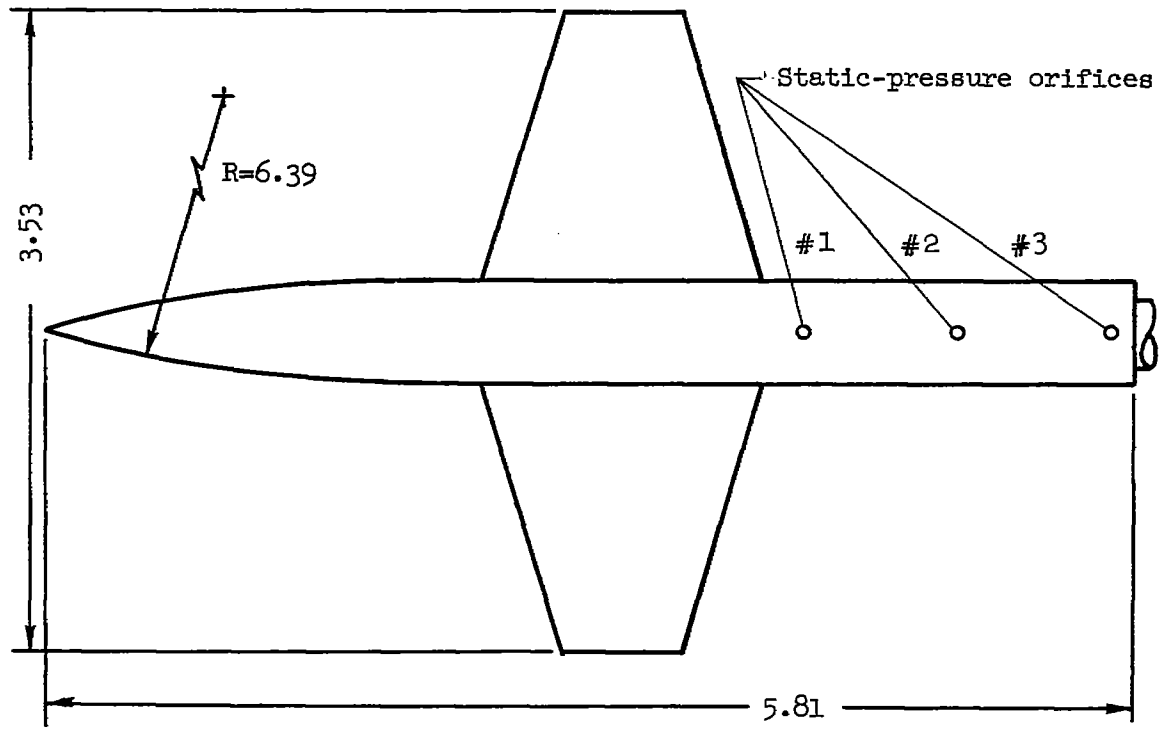

(b) Large wing-body model.

Figure 3.- Models used to evaluate wall interference.

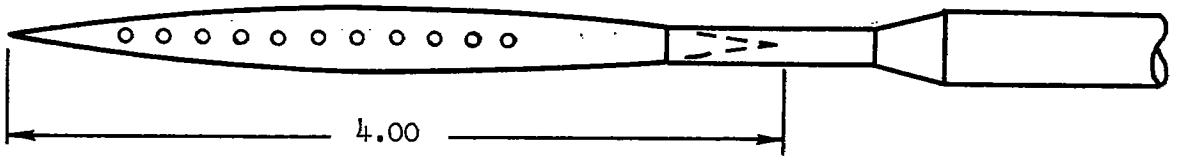

(c) RM 12, maximum diameter 0.333.

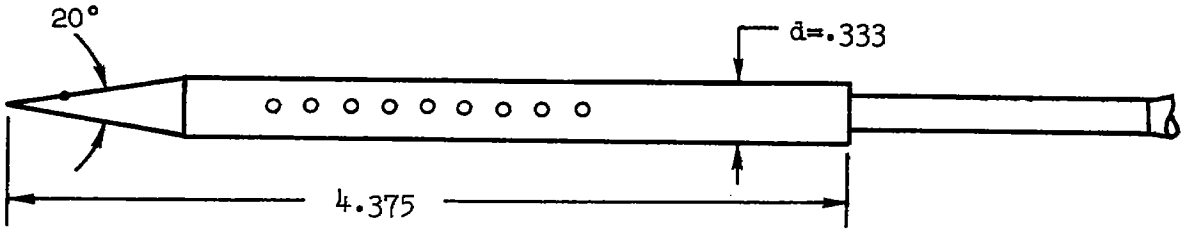

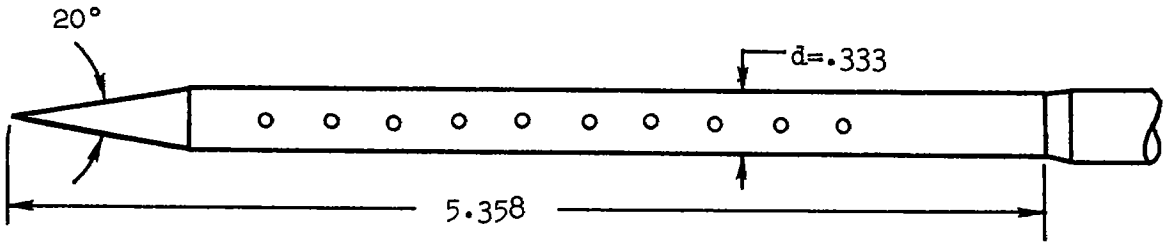

(d) Cone cylinders.

Figure 3.- Concluded.

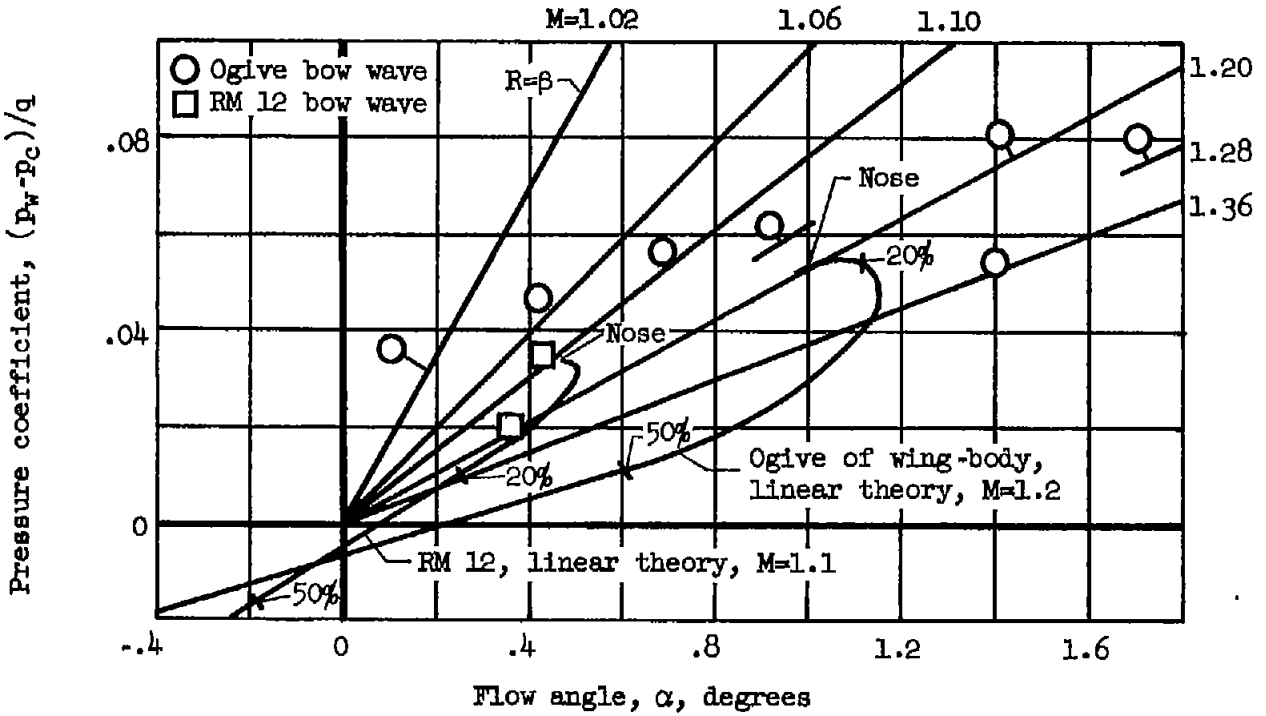

Figure 4.- Permeability requirements for various disturbance fields.

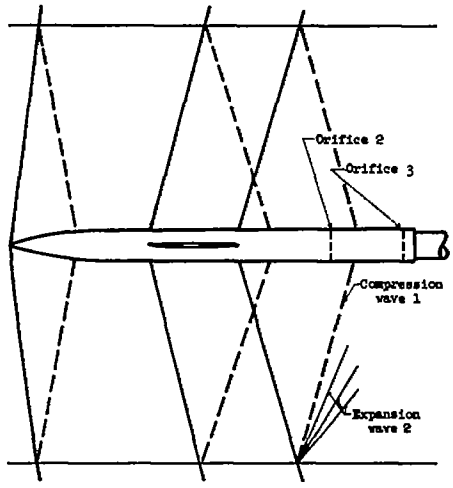

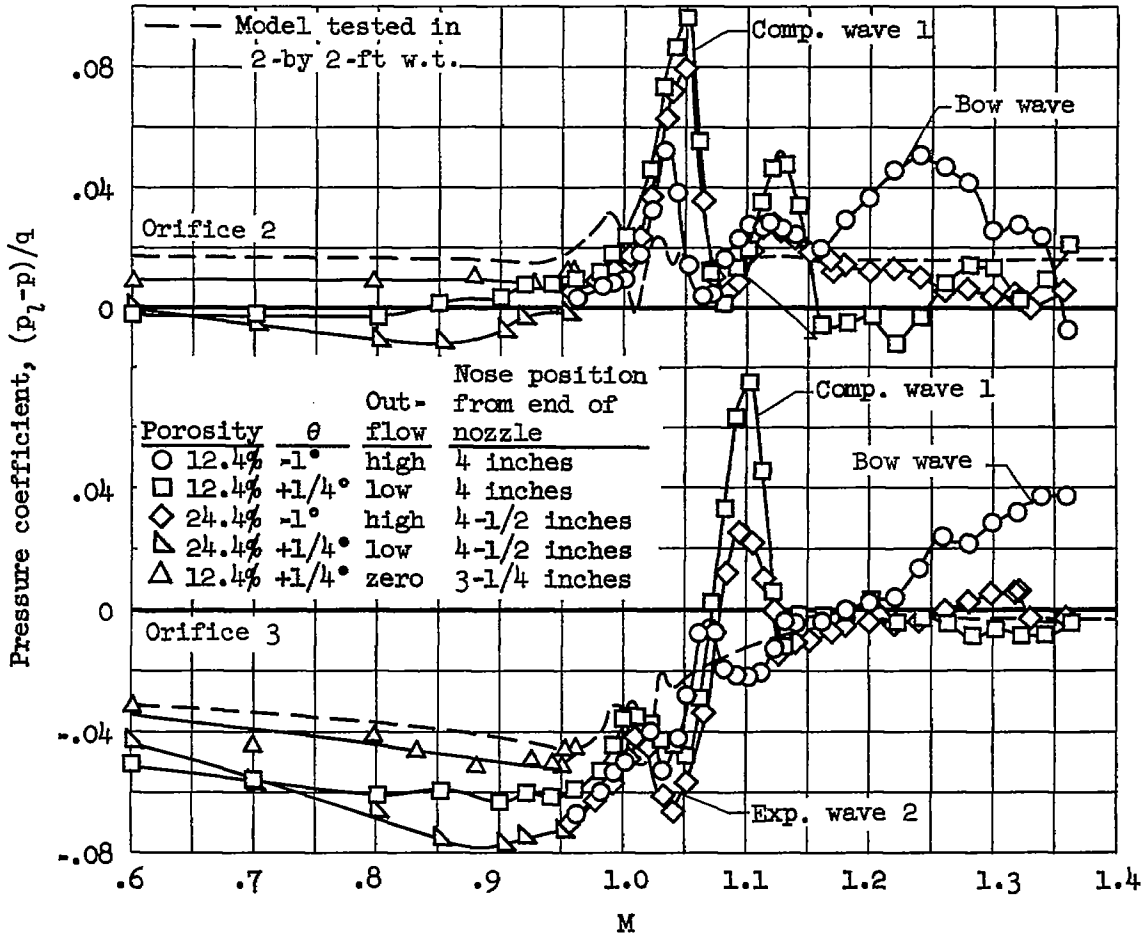

Figure 5.- Typical plots of pressure coefficient against Mach number for the small wing-body model.

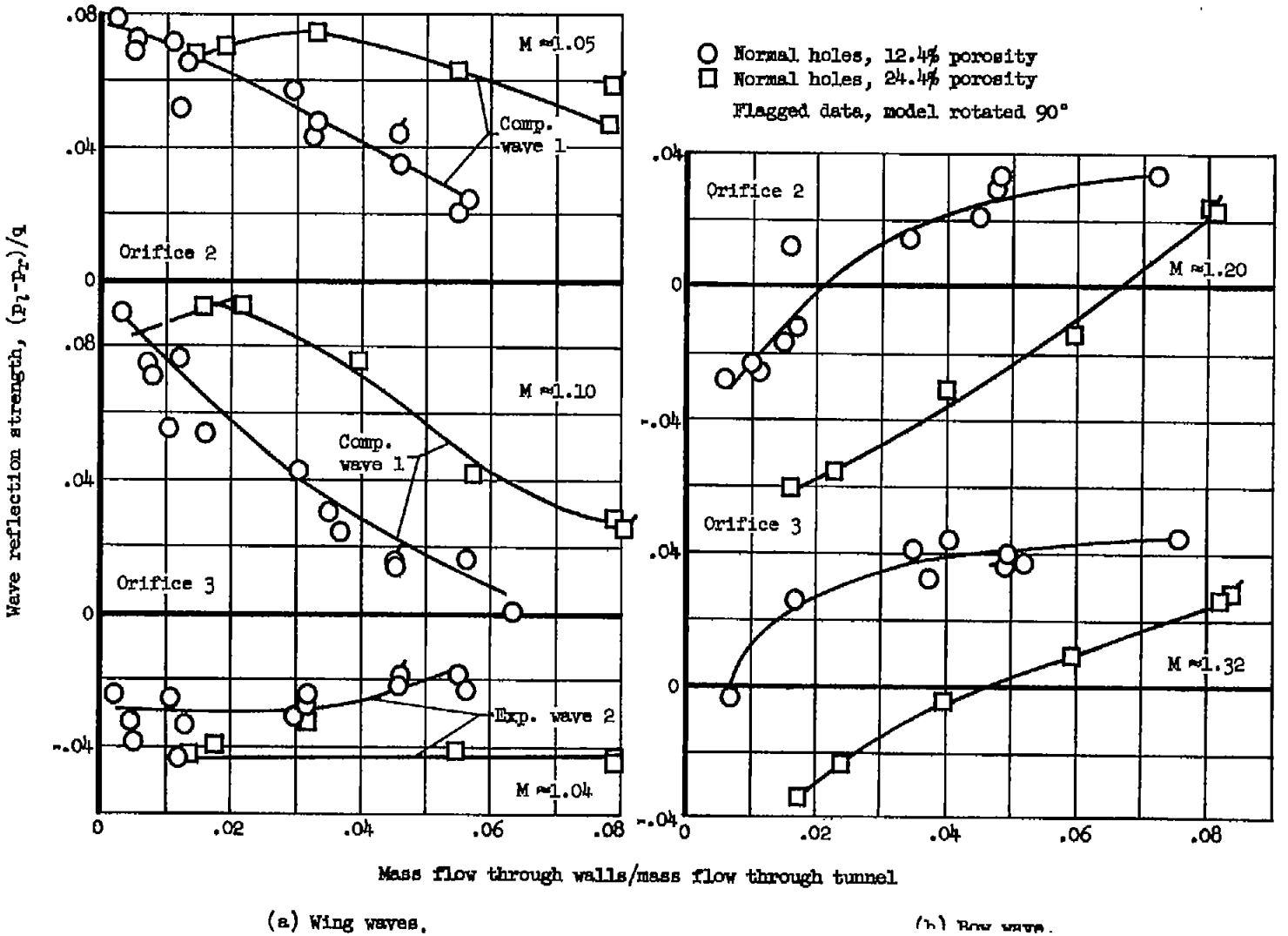

(a) Wing waves.

(b) Bow wave.

Figure 6.- Effect of outflow and porosity on wave reflection for the small wing-body model.

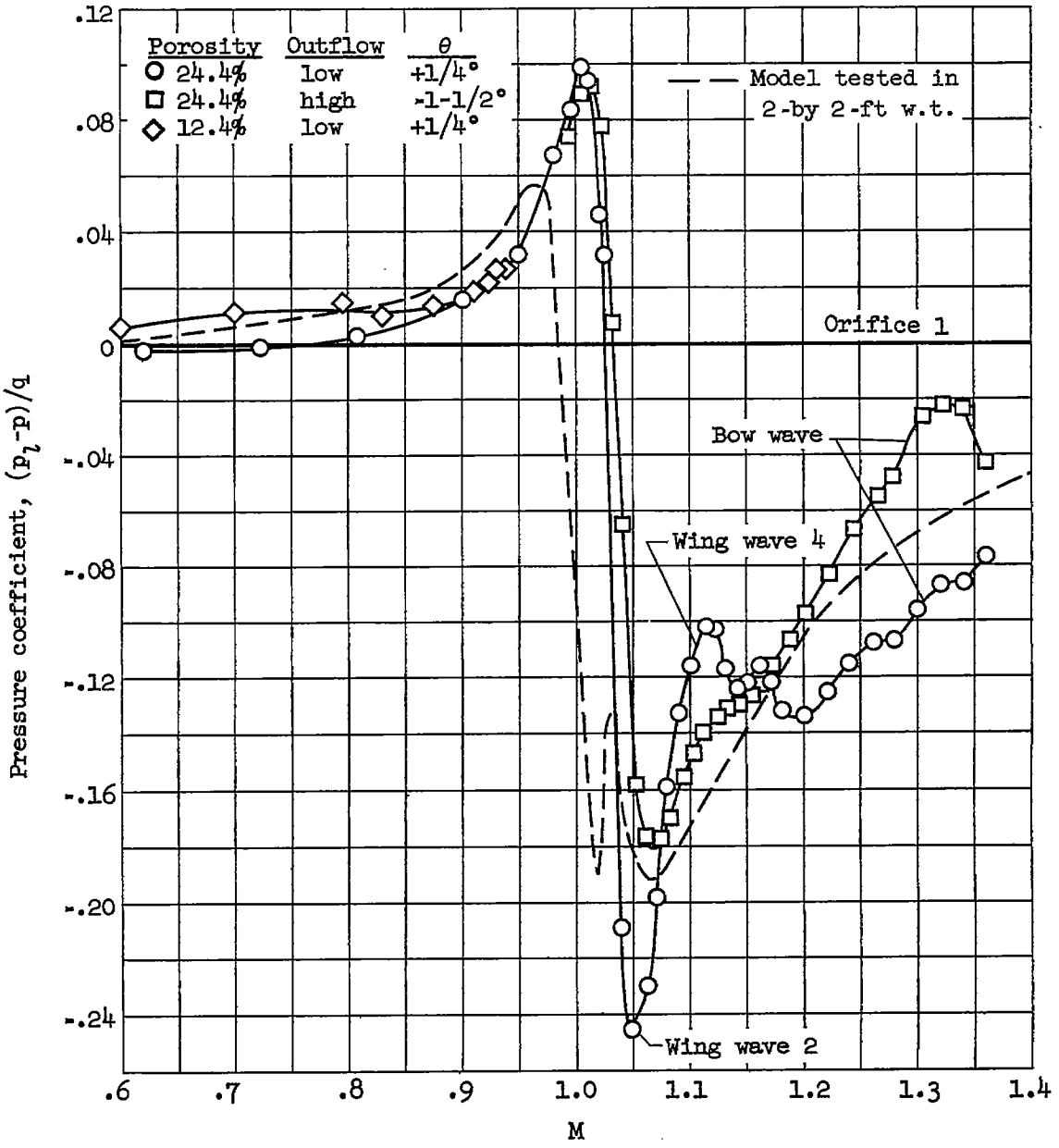

(a) Orifice 1.

Figure 7.- Typical plots of pressure coefficient against Mach number for the large wing-body model.

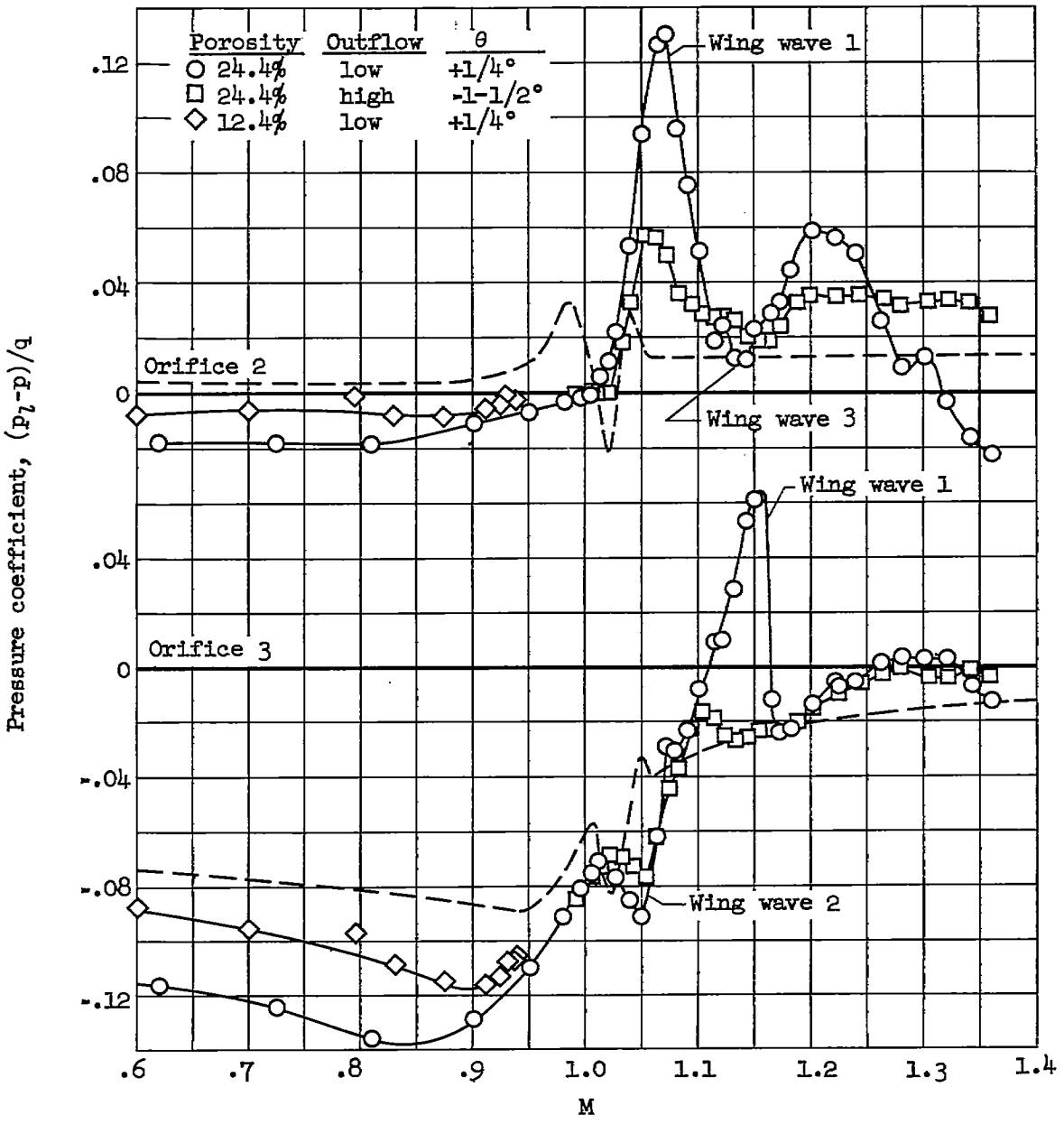

(b) Orifices 2 and 3.

Figure 7.- Concluded

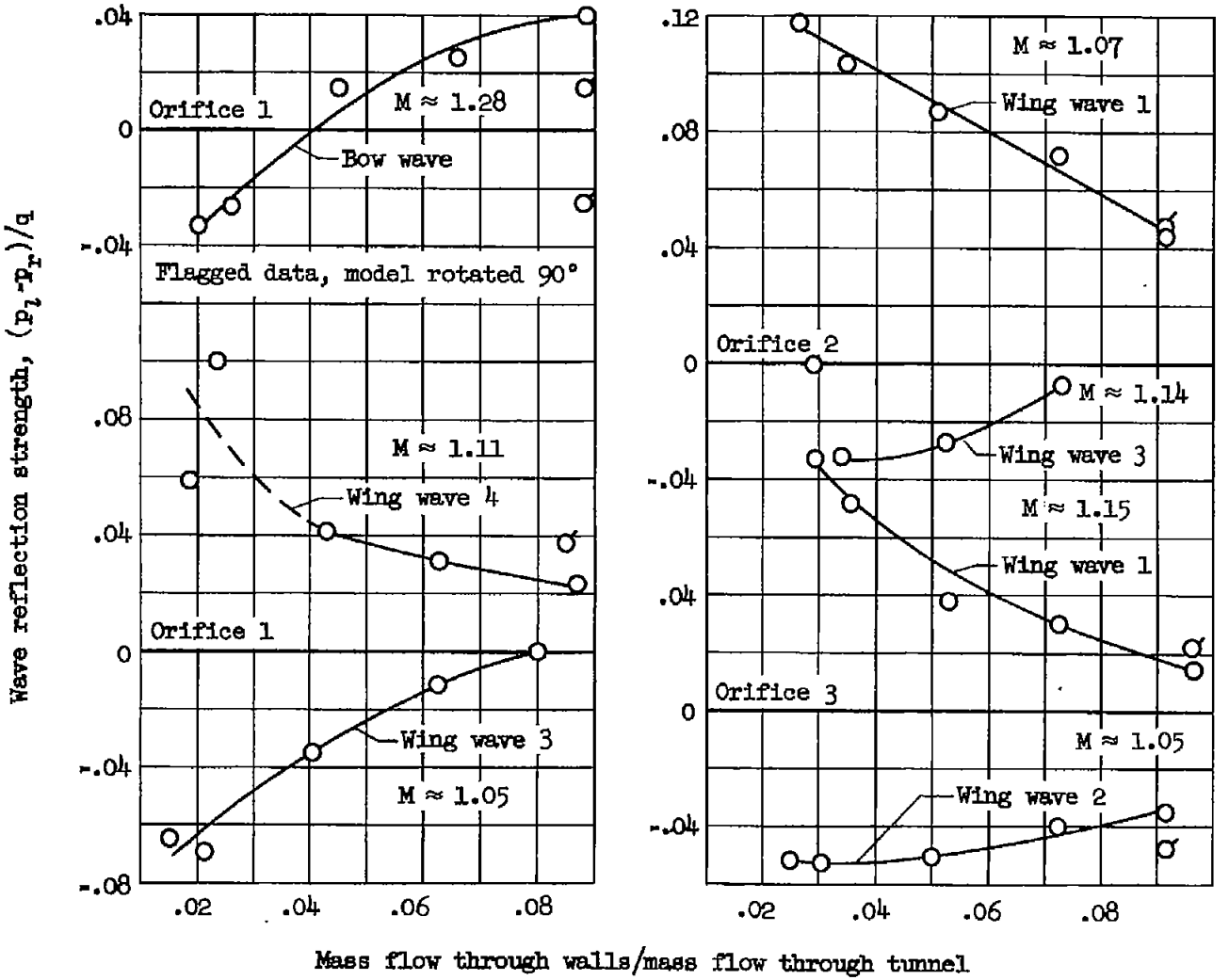

Figure 8.- Effect of outflow on wave reflection for the large wing-body model; thin walls, normal holes, 24.4-percent porosity.

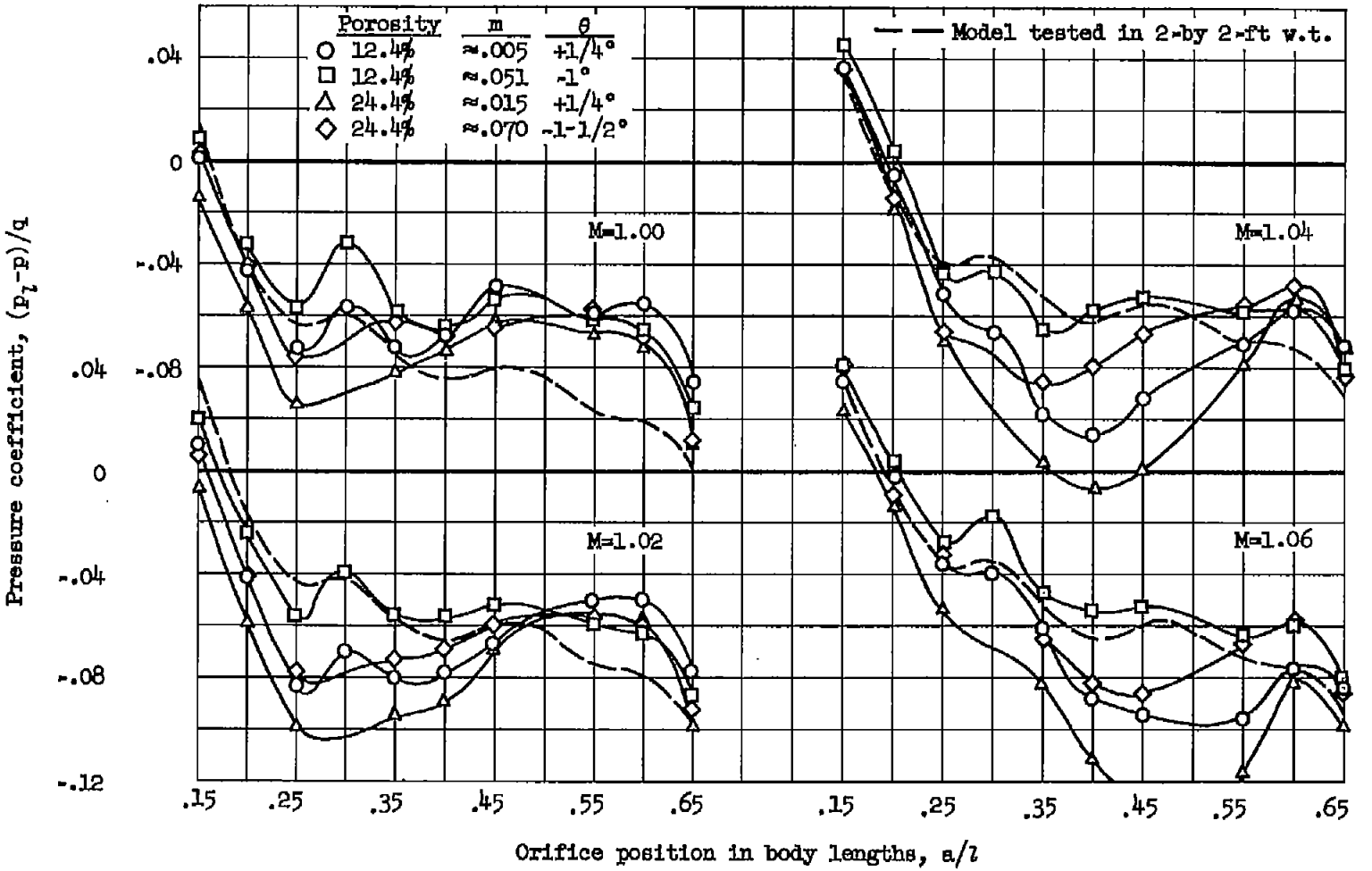

(a) M=1.00 to M=1.06

Figure 9.- Effect of outflow and porosity on the pressure distribution over the RM 12 body of revolution at supersonic speeds; thin walls, normal holes.

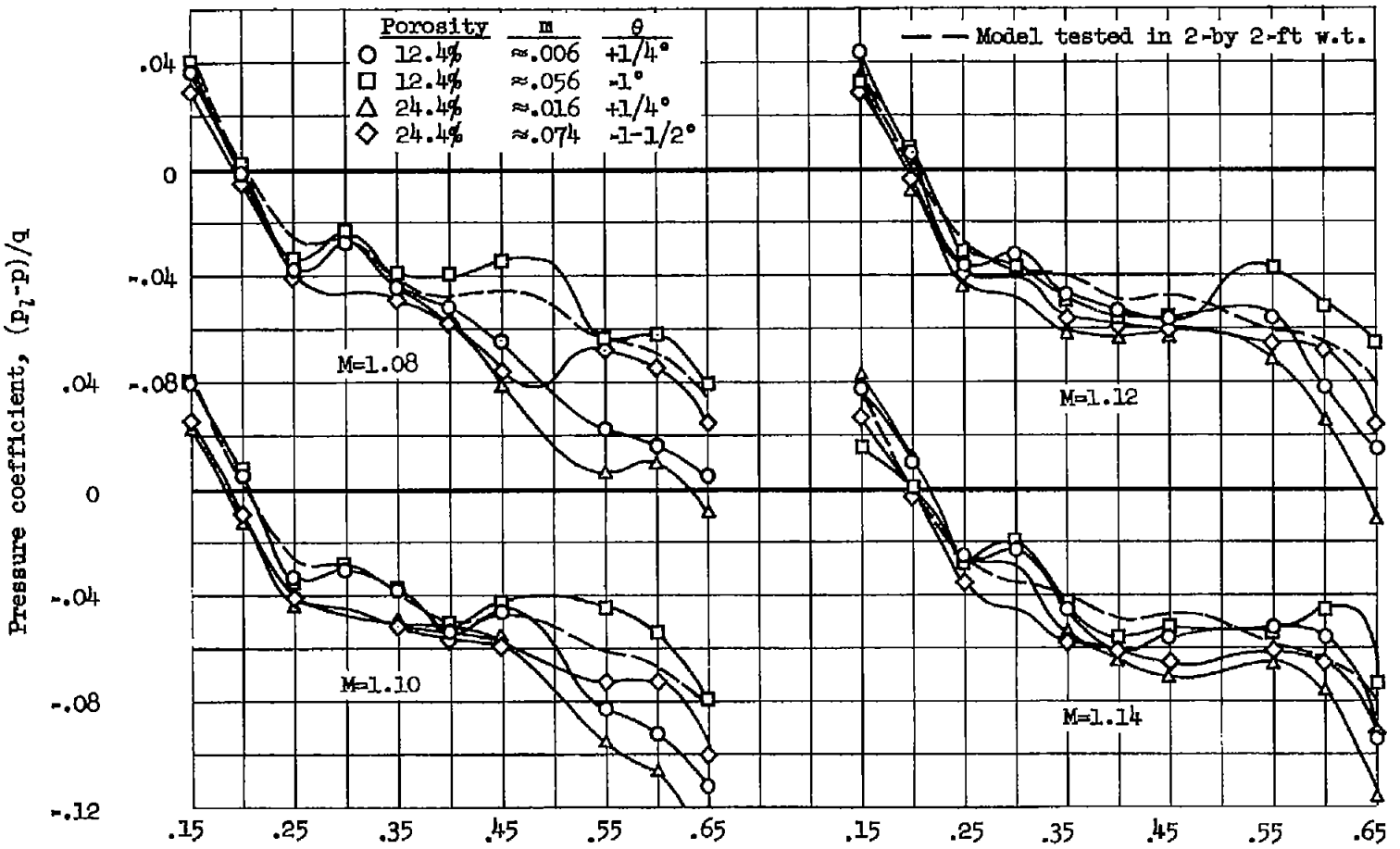

(b) M=1.08 to M=1.14

Figure 9.- Concluded.

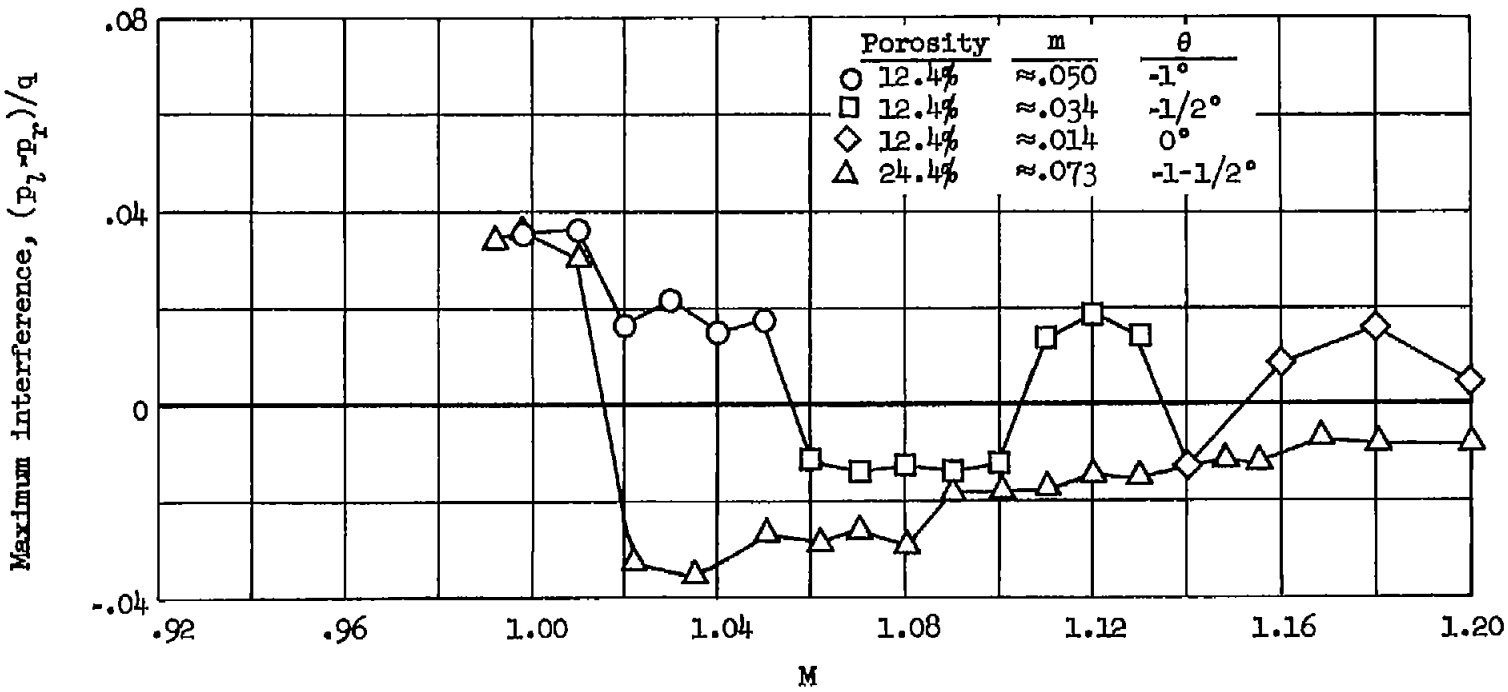

Figure 10.- Effect of outflow and porosity on the maximum interference over the RM 12 body of revolution as a function of Mach number; thin walls, normal holes.

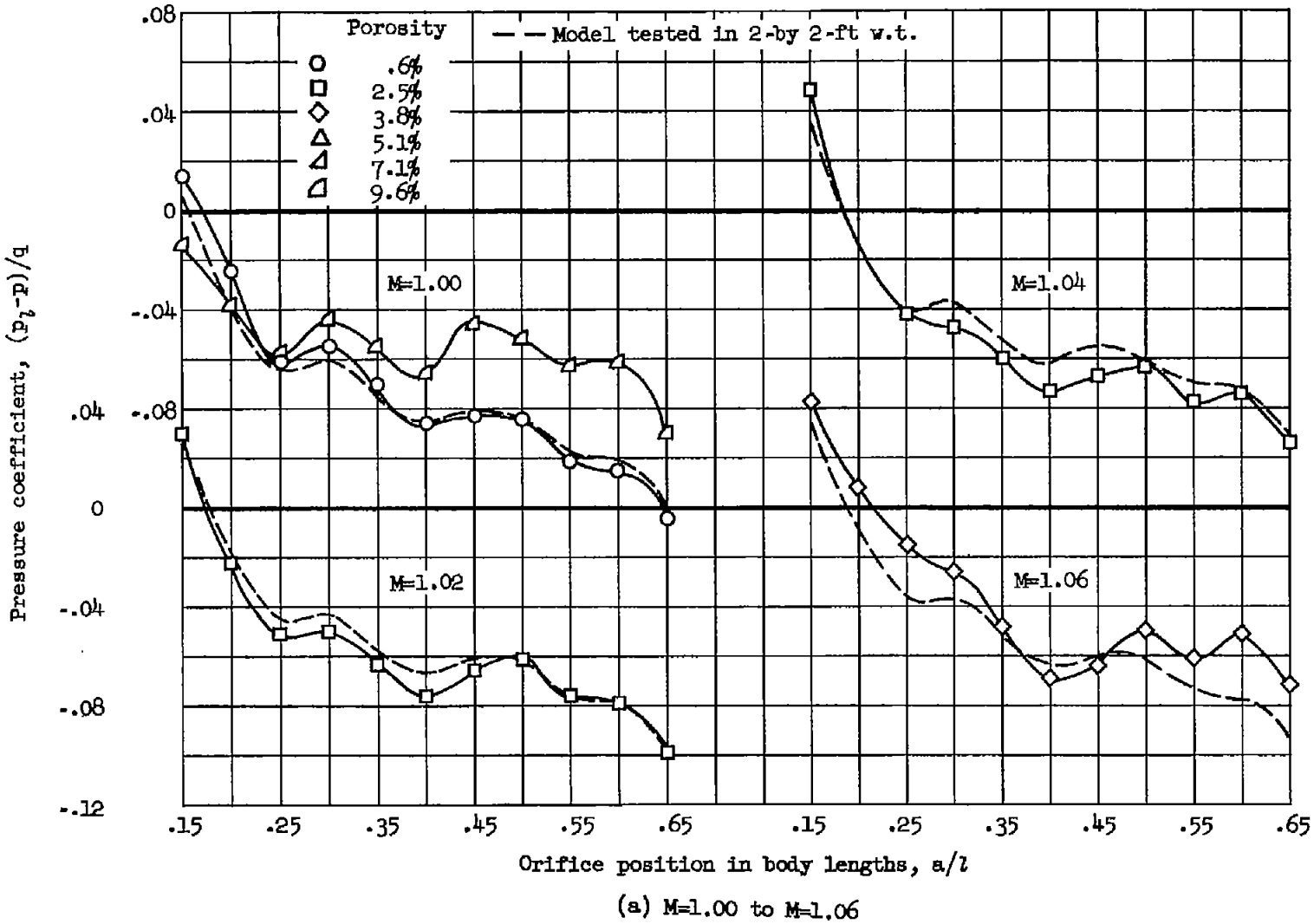

(a) M=1.00 to M=1.06

Figure 11.- Effect of porosity at constant low outflow on the pressure distribution over the RM 12 body of revolution at supersonic speeds; normal holes, thick walls, $m<0.1$, $\theta = +1/4^{\circ}$.

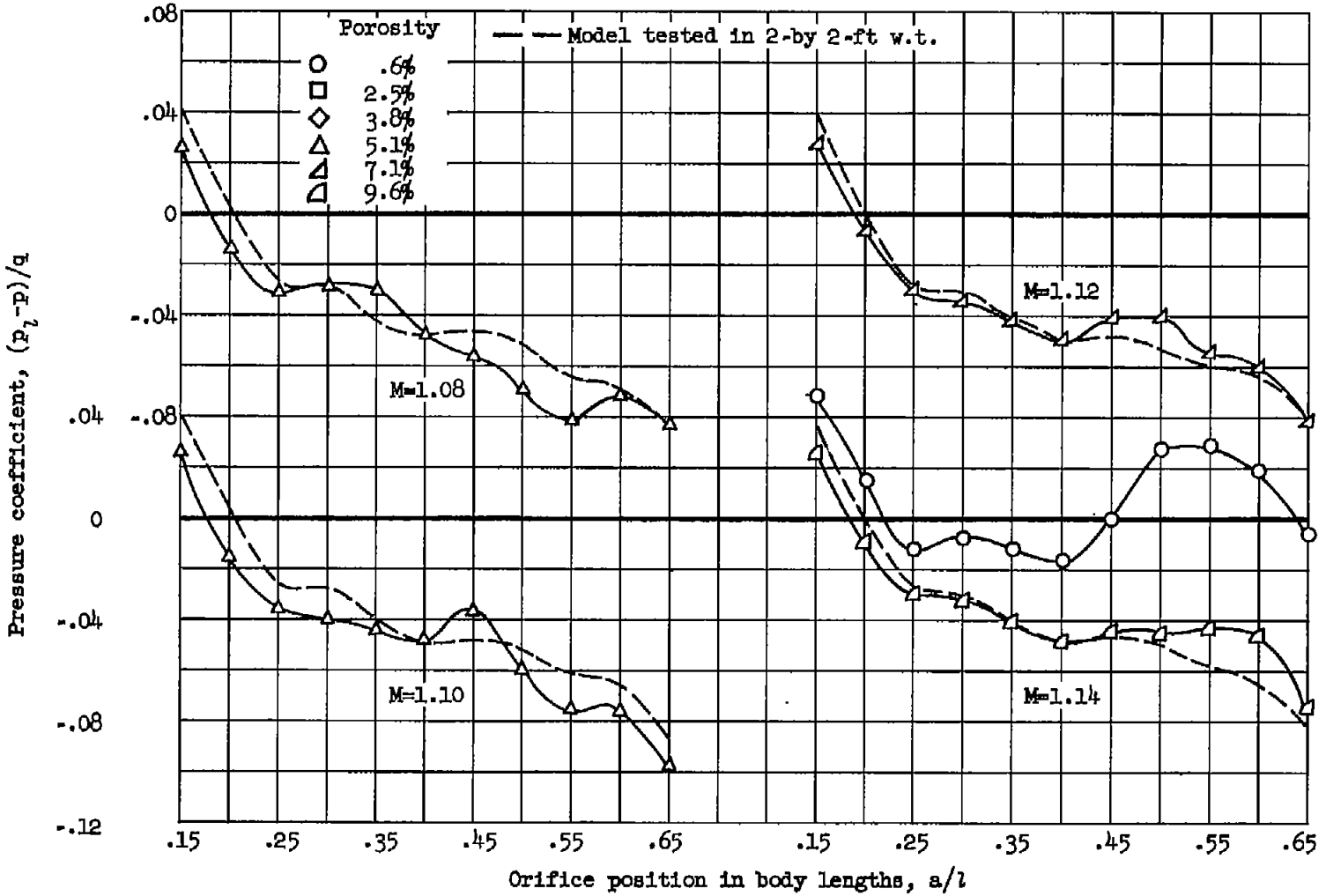

(b) M=1.08 to M=1.14

Figure 11.- Concluded.

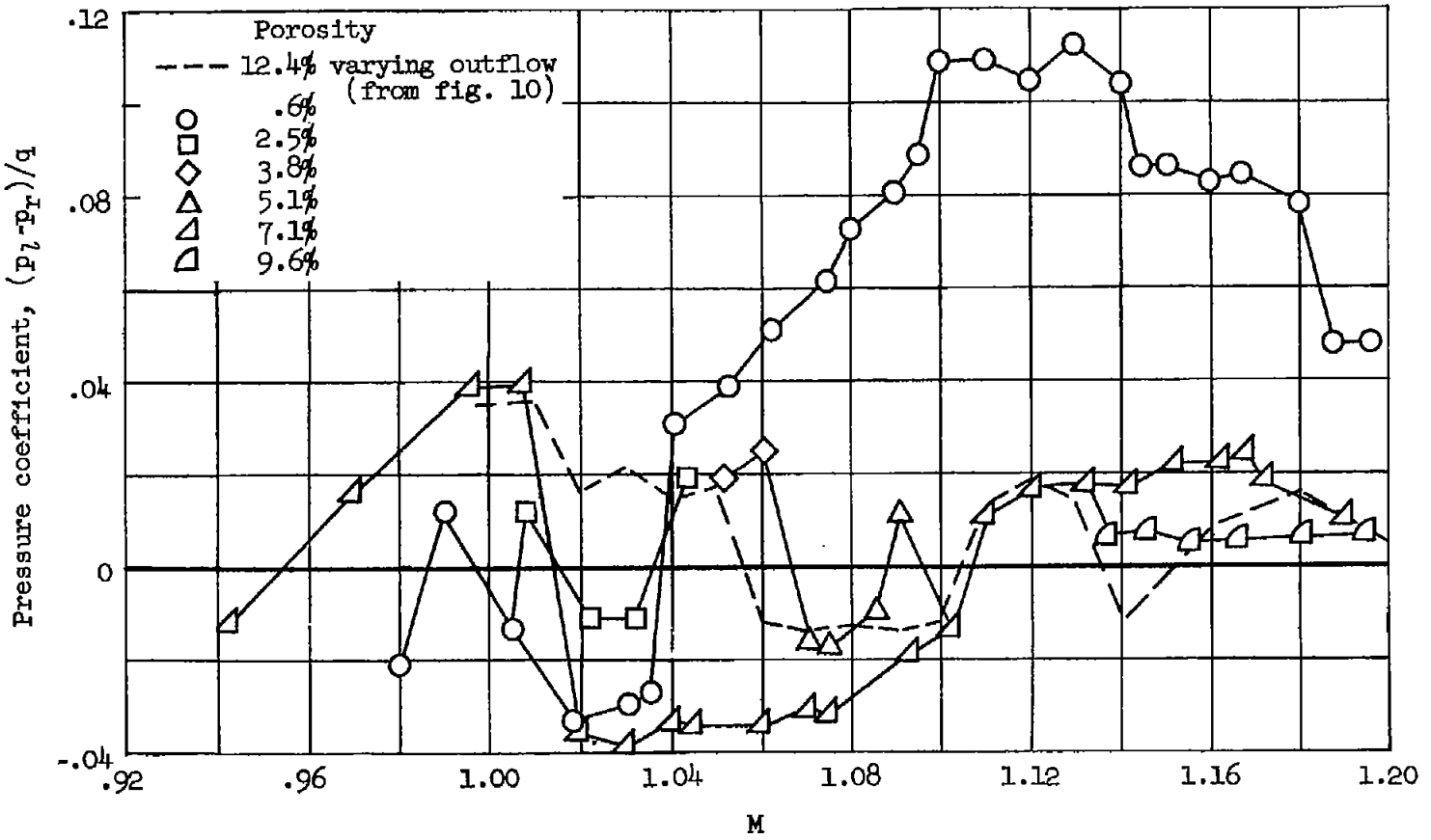

Figure 12.- Effect of porosity at constant low outflow on the maximum interference over the RM 12 body of revolution as a function of Mach number.

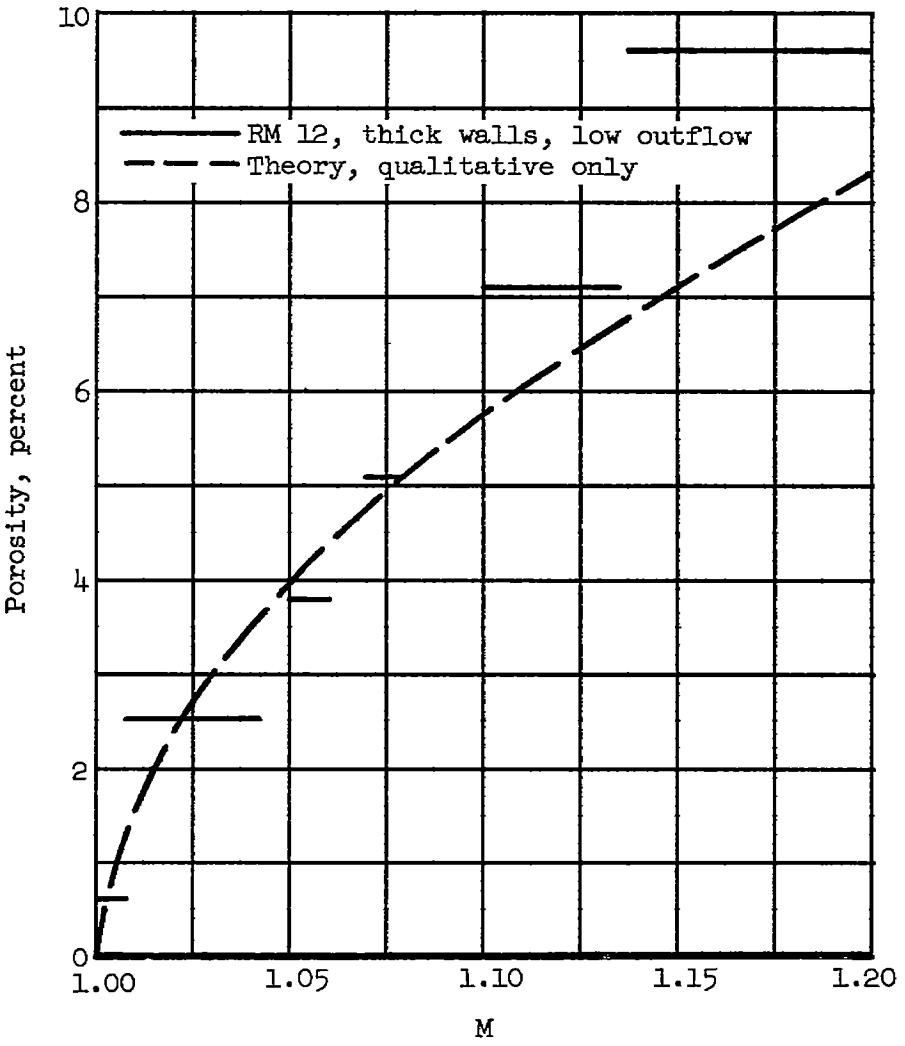

Figure 13.- Porosity variation with Mach number for minimum interference on the RM 12.

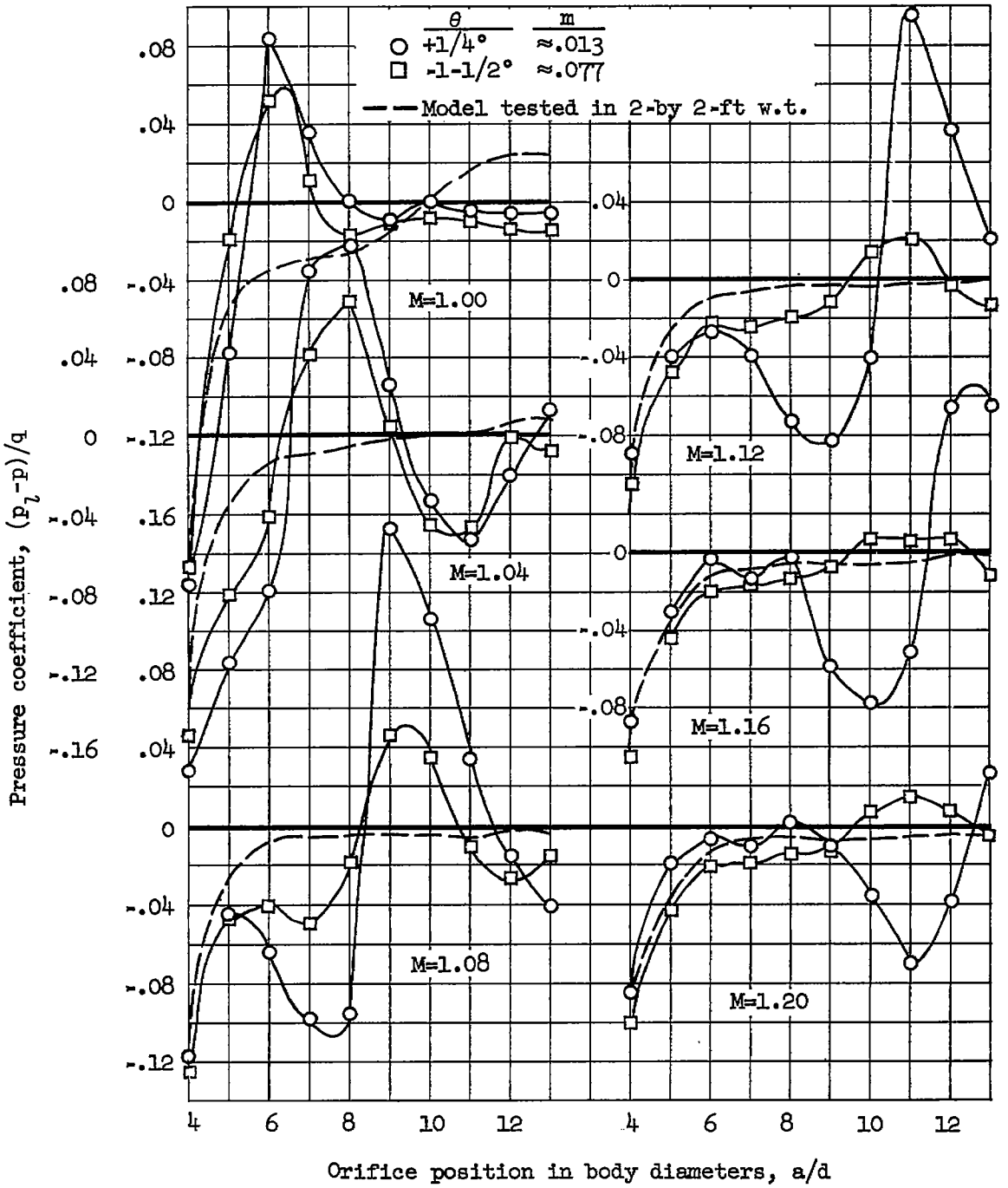

Figure 14.- Effect of outflow on the pressure distribution over the cone-cylinder body for the 24.4-percent-porosity walls at supersonic speeds; normal holes, thin walls.

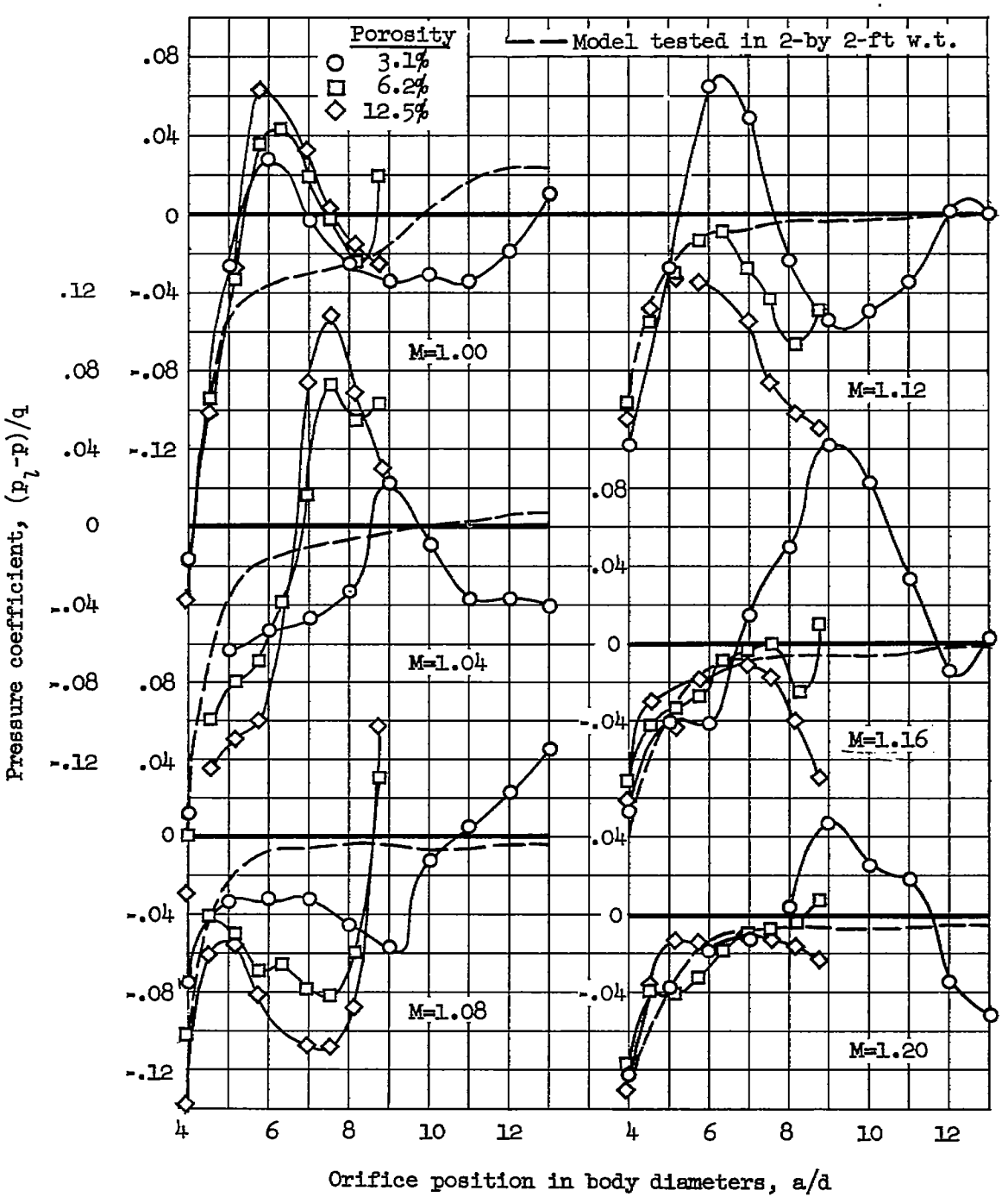

Figure 15.- Effect of porosity on the pressure distribution over the cone-cylinder body at supersonic speeds; slant holes, thin walls, $\theta = 0^{\circ}$, $m \approx 0.018$.